Multifunctional structures with quasi-solid-state Li-ion battery cells and sensors for the next generation climate neutral aircraft

Horizon Europe | HORIZON-CL5-2021-D5-01-05

Greenhouse gas aviation emissions reduction technologies towards climate neutrality by 2050

D2.1 - Interim report on electrochemical material selection, initial cell design, on-cell sensor development

This project receives funding from the European Union's Horizon Europe research and innovation programme under grant agreement no. 101056674 (MATISSE)

Deliverable No.	D2.1	
Deliverable Title	Interim report on electrochemical material selection, initial cell design, on-cell sensor development	
Deliverable Type	Report	
Dissemination level	Sensitive	
Written By	Mintao Wan, Dominic Bresser (KIT-HIU) Alexander Beutl (AIT) Roberto Simmarano (SENSICHIPS)	13.08.2023
Checked by	Roberto Simmarano (SENSICHIPS)	14.09.2023
Approved by	Helmut Kühnelt (AIT)	19.09.2023
Status	Final	19.09.2023

REVISION HISTORY

Version	Date	Who	Change
V1	19.09.2023		

TABLE OF CONTENTS

PROJECT ABSTRACT

MATISSE responds to the fourth bullet of the HORIZON-CL5-2021-D5-01-05 topic "expected outcome", delivering improved aircraft technologies in the area of multifunctional structures capable of storing electrical energy for hybrid electric aircraft applications. This consists in integrating Li-Ion cells into aeronautical composite structures, sharing the load-bearing function with the structure and achieving an aircraft structural element capable of functioning as a battery module.

To do so, MATISSE will:

- advance Li-Ion battery cell technology, in a non-conventional formulation suitable for bearing structural loads: NMC811 (cathode), Si/C (anode) and bi-continuous polymer-ionic quasi-solid-state electrolyte (BCE), i.e. NMC811|BCE|Si/C, achieving 170-270 Wh/kg at cell level;
- enable the functional integration of Li-Ion cells into solid laminate and sandwich composite structures;
- make the structural battery smart, by equipping it with on-cell and in-structure sensors, connected to a chip-based CMU (battery Cell Monitoring Unit) and PLC (Power Line Communication).

MATISSE delivers a multifunctional structure demonstrator capable of power delivery, power management and safety monitoring. This consists of a full-scale wing tip (1.42 m × 0.69 m) for use in place of the current wingtip assembly installed on Pipistrel Velis Electro, embedding a module of 40 battery cells at 72 VDC. This will undergo a comprehensive testing and characterisation campaign, qualifying the technology at TRL 4 at the end of the project (2025). MATISSE will also encompass aspects related to flight certification, life-cycle sustainability and virtual scale-up, paving the way towards the application of structural batteries as an improved performance key enabling technology for next generation commuter and regional hybrid electric aircraft applications.

The strong and complementary consortium of 8 partners from 5 different European countries and one associated partner country representing industrial companies, SMEs and RTOs is coordinated by AIT Austrian Institute of Technology. MATISSE is scheduled to run from September 1st 2022 to August 31st 2025, for a total duration of 36 months and has received funding from the European Union's Horizon Europe research and innovation programme under Grant Agreement no. 101056674. A full list of partners and funding can be found at: https://cordis.europa.eu/project/id/101056674.

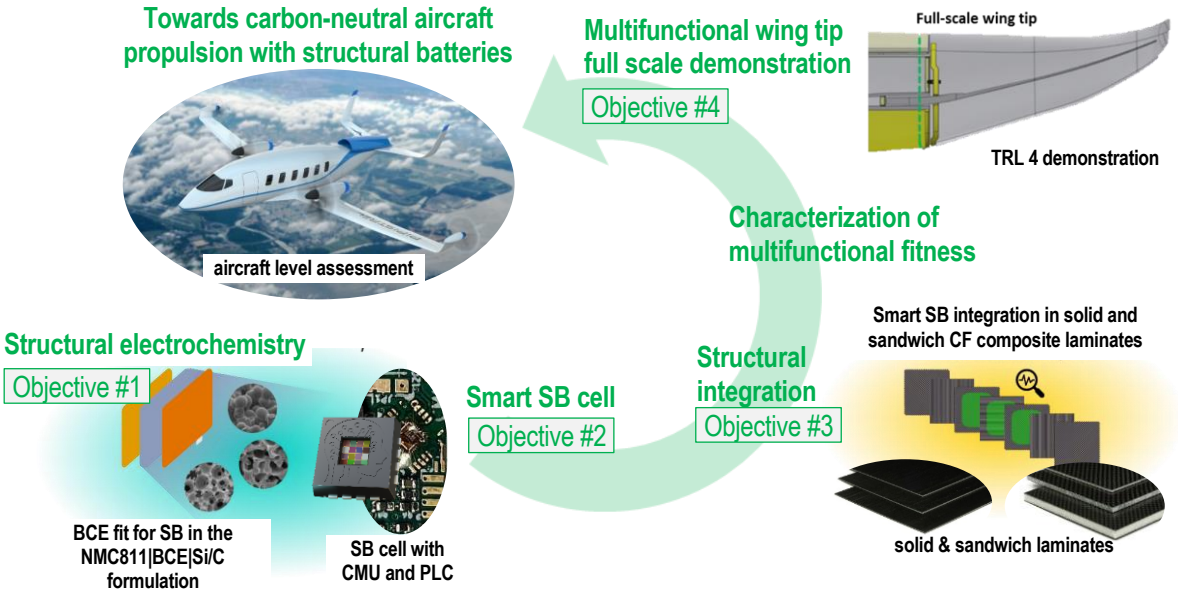

Figure 1. MATISSE concept overview.

LIST OF ABBREVIATIONS

Acronym / Short Name	Meaning
C45	Super C45 carbon additive
CMU	Cell monitoring unit
FT-IR	Fourier-transform infrared spectroscopy
LATP	Lithium aluminum titanium phosphate
Li	lithium
LiFSI	Lithium-bis(fluorosulfonyl)imide
NMC811	$LiNi_{0.8}Mn_{0.1}Co_{0.1}O_2$
NMP	*N*-Methyl-2-pyrrolidone
PVdF	polyvinylidene difluoride
PVdF-HFP	Poly(vinylidene fluoride-co-hexafluoropropylene)
PVdF-TrFE	Poly(vinylidene fluoride-co-trifluoroethylene)
$PYR_{13}FSI$	*N*-Propyl-*N*-methylpyrrolidinium bis(fluorosulfonyl)imide
$PYR_{13}TFSI$	1-Butyl-1-methylpyrrolidinium bis(trifluoromethylsulfonyl)imide
SB	Structural battery
SPLC	Power line communication
TGA	Thermogravimetric analysis

EXECUTIVE SUMMARY

In the frame of Task 2.1, a series of electrodes (NMC cathode, composited NMC cathode, Si/graphite anode, and composited graphite anode) with the different electrolytes (gel electrolyte, and hybrid electrolyte) were characterized at the full-cell level (cyclic voltammetry, cycling tests). Initially, the compatibility of the electrodes with the hybrid electrolyte system was relativity poor compared to the gel electrolyte but had been further improved through an anode-electrolyte interface protection method.

Apart from the compatibility testing between the electrode and electrolyte at the coin-cell level, we scaled-up the electrode and electrolyte to a much larger cell level. Composite NMC electrode, composite graphite anode, gel electrolyte and semi-solid electrolyte were employed in the pouch cells with nominal capacities of 70 mAh (single layer), 140 mAh (double layer), and 280 mAh (4-layer). The safety, influence of moisture, and repeatability issues during cell scale-up were also taken into consideration. In addition, the incorporation of the CMU-I unit and SPLC system in the multi-layer pouch cells is also in progress.

1. INTRODUCTION

The primary objectives of WP2 involve the improvement of multifunctional semi-solid-state batteries, which encompasses enhancements of the structural battery electrochemistry, cell design, processing, and scaling. Additionally, WP2 also aims at integrating the cell monitoring unit (CMU) and a novel power line communication (SPLC) system into the battery architecture, and at manufacturing smart SB cells which would be delivered to WP4 eventually.

2. ELECTRODE DEVELOPMENT (AIT)

2.1. CATHODE DEVELOPMENT

For the electrode preparation, a lab-scale processing routine has been employed using a centrifugal planetary mixer (THINKY ARE-250). The slurry (recipe in Table 1) was further cast on Al foil and properly dried. No post-processing was conducted (e.g. calendaring).

Table 1. Recipe of the NMC cathode.

	NMC811 [wt.%]	PVdF [wt.%]	C45 [wt.%]	Solvent
Cathode	90	5	5	NMP

The NMC811 electrodes were tested in 2016-coin cell setups using Li metal as counter electrode and a gel electrolyte (PVdF-HFP+0.4LiFSI-0.6PYR_{13}FSI+SiO_2 (6 vol.%)) as separator. The electrode discs (15 mm diameter, ~1.7 cm^2) were previously wetted with around 50 µL of the 0.4LiFSI-0.6PYR_{13}FSI ionic liquid electrolyte before cell assembly. A current density of 0.1 mA/cm^2 was applied during testing, i.e. approx. C/10 in GCPL mode (Figure 2a). Promising results for the NMC811 half-cells were obtained with discharge capacities of up to 190 mAh/g_{NMC811}, similar to the performance in conventional liquid electrolyte (Figure 2b). However, low Coulombic efficiencies were encountered as well as some cycling stability issues, which are expected to result from the electrolyte and the Li metal anode rather than from the cathode.

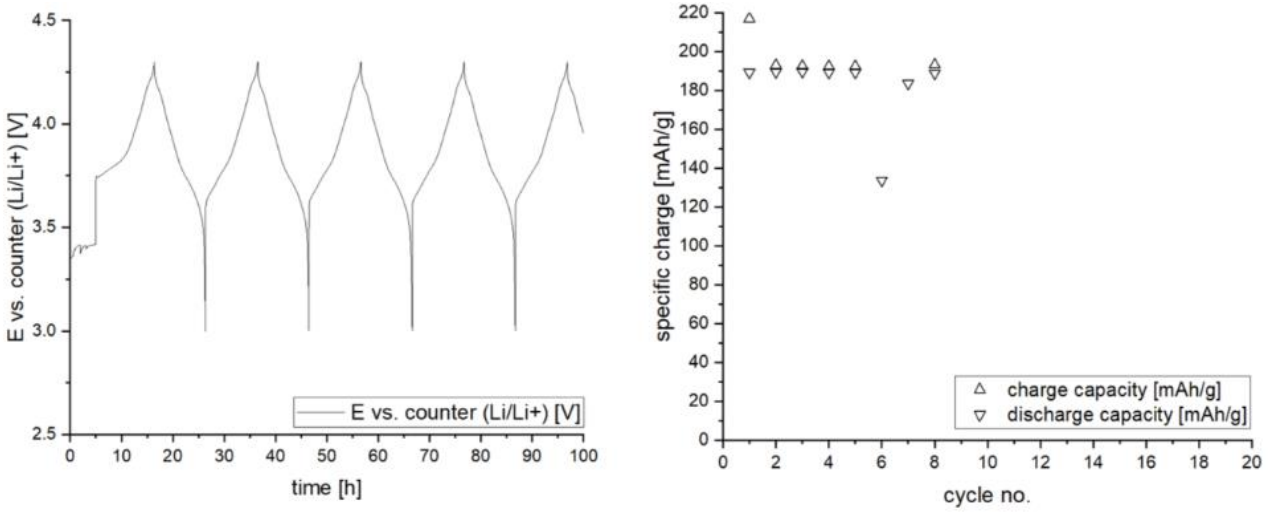

Figure 2. Left, potential profile of NMC811 half-cells tested at C/10 (GCPL); right, corresponding specific charge vs. cycle number plot.

Furthermore, AIT is focusing on the development of feasible strategies to incorporate the electrolyte into the cathode and anode composites using 3M LiFSI in $PYR_{13}FSI$ + PVdF-HFP as a model electrolyte. The recipe in Table 2 has been used for the composite NMC811 cathode.

Table 2. Recipe of the composite NMC cathode.

	NMC811 [wt.%]	PVdF-HFP [wt.%]	C45 [wt.%]	Ionic liquid electrolyte [wt.%]
Cathode	69.4	7.3	4.9	18.5

2.2. ANODE DEVELOPMENT

For the anode preparation, a lab-scale processing routine has been employed using a centrifugal planetary mixer (THINKY ARE-250). The slurry was further cast on Cu foil and properly dried. As binder, different materials were tested, i.e. alginic acid (AA), polyacrylic acid (PAA), carboxymethyl cellulose (CMC), and a mixture of PAA and CMC. The general recipe is given in Table 3.

Table 3. Recipe of the composite Si/graphite anode.

	Si+Graphite (Si/C) [wt.%]	Binder [wt.%]	C45 [wt.%]	Solvent
Anode	90	5	5	H_20

For the Si/C composite electrodes, the same cell setup and testing protocol as for the NMC811 electrodes was used (Figure 3). Good results were also obtained for the Si/C composite electrodes with up to 647 mAh/$g_{Si/C}$ for the electrodes using CMC as binder. Similar to the tests

conducted with the cathodes, some stability issues were encountered, which probably result from the Li metal anode.

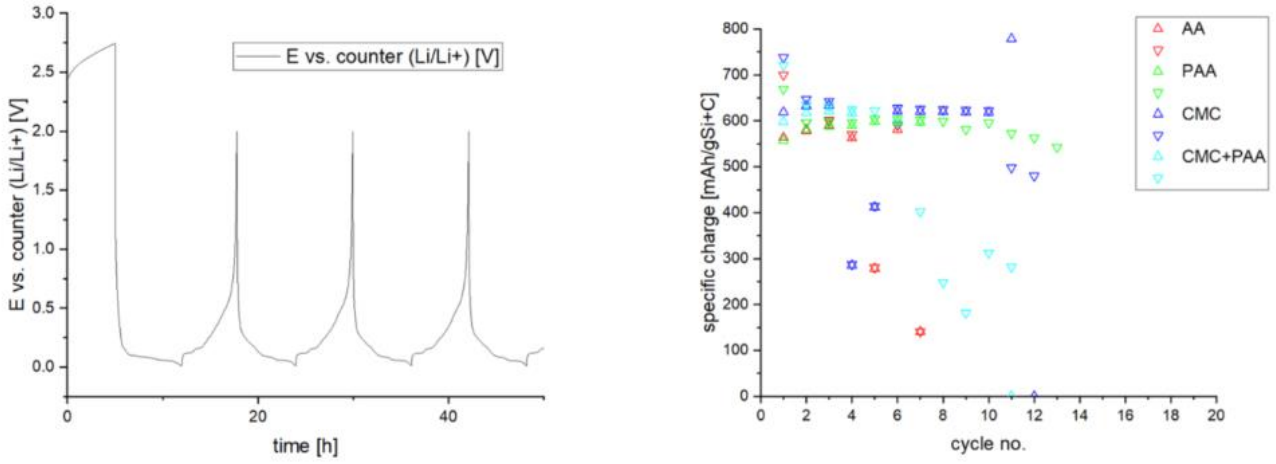

Figure 3. Left, potential profile of Si/C composite electrode half-cells tested at C/10 (GCPL); right, corresponding specific charge vs. cycle no. plot for different binder materials (triangles pointing up – charge; triangles pointing down – discharge).

Composite graphite anodes using 3M LiFSI in $PYR_{13}FSI$ + PVdF-HFP as a model electrolyte were also prepared. The recipe in Table 4 was used for the composite graphite anode:

Table 4. Recipe of the composite graphite anode.

	Graphite [wt.%]	PVdF-HFP [wt.%]	C45 [wt.%]	Ionic liquid electrolyte [wt.%]
anode	44.8	10.9	5.8	38.5

2.3. SCALABILITY OF COMPOSITE ELECTRODE PRODUCTION

Around 400 g batches of the composite anode, composite cathode, and gel electrolyte were prepared for casting on the AIT-pilot line (Figure 4). Surface-treated Cu foil and conventional Al foil was used as substrate for the composite anode and composite cathode, respectively. The gel electrolyte was cast on Al foil as well. All casts worked well and good processability was observed for all components. However, some compatibility issues were encountered, and gel-like agglomerates formed. These could be removed by sieving the slurries before further use. A roll-to-roll coating process was still possible. The rolled coatings could not be properly dried, though. Therefore, the different coatings were first unwound and cut into tapes of around 40 cm length for proper drying at 80 °C for 2-3 days. Thereafter, the different components could be cut into the 100 x 70 mm^2 pouch cell shape and manually calendared in the dry room.

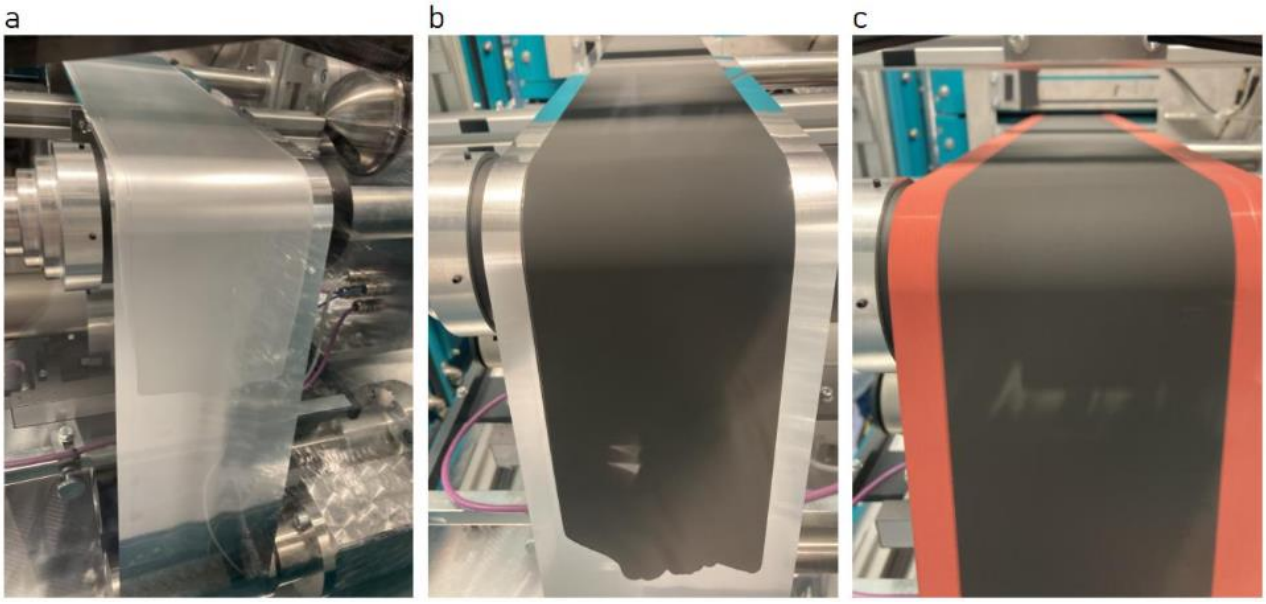

Figure 4. a, Gel electrolyte, b, composite cathode, c, composite anode prepared on the AIT-pilot line.

2.4. RELIABILITY AND SCALABILITY TESTS FOR ELECTRODE PREPARATION

Reliability studies on the electrode manufacturing were conducted. After measurements in coin cells, pouch cells were prepared and investigated for their performance. The gel electrolyte (3M LiFSI in $PYR_{13}FSI$ + PVdF-HFP; 70:30 vol.%; + SiO_2; 7 vol.%; 40 µm) was sandwiched between the composite anode and cathode electrodes and the cell was sealed in a pouch foil under vacuum. The assembled cells were then tested by GCPL using different C rates. As can be seen in Figure 5 the reproducibility of the results was high. However, the specific charge values were very low. Only around 20 mAh/g_{NMC811} could be obtained at rather low C rates of C/10. Compared to the performance in coin cells (~120 mAh/g_{NMC811}) the poor performance in pouch cells was unexpected. Possible reasons seem to be the different pressure applied during cycling. In previous studies, we determined the pressure in coin cells to be around 2 bar, whereas it is only around 1 bar for the pouch cells (as they were sealed under vacuum). In order to mitigate this issue, the pouch cells were hot-calendared at 100 °C after cell assembly to improve the contact between all layers. Then the cells were sealed again and tested. Figure 6 shows that the performance of the pouch cells was significantly improved after hot-calendaring reaching capacity values up to 100 mAh/g_{NMC811} at C rates of C/10, thus approaching the performance of coin cells. This results highlight the importance of a good contact between the individual layers of the cell.

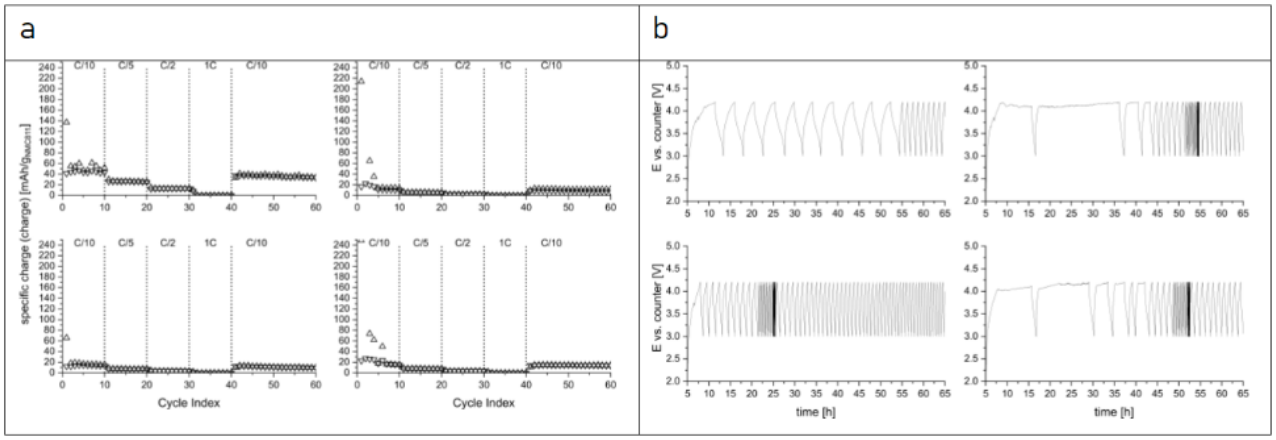

Figure 5. Rate capability tests of 4x 100 x 70 mm² pouch cells using the developed composite cathode and anodes. GCPL at 3.0-4.2 V vs. Li^+/Li were used and C rates of C/10, C/5, C/2, 1C with respect to the nominal loading of the composite cathode (~1mAh/cm²).

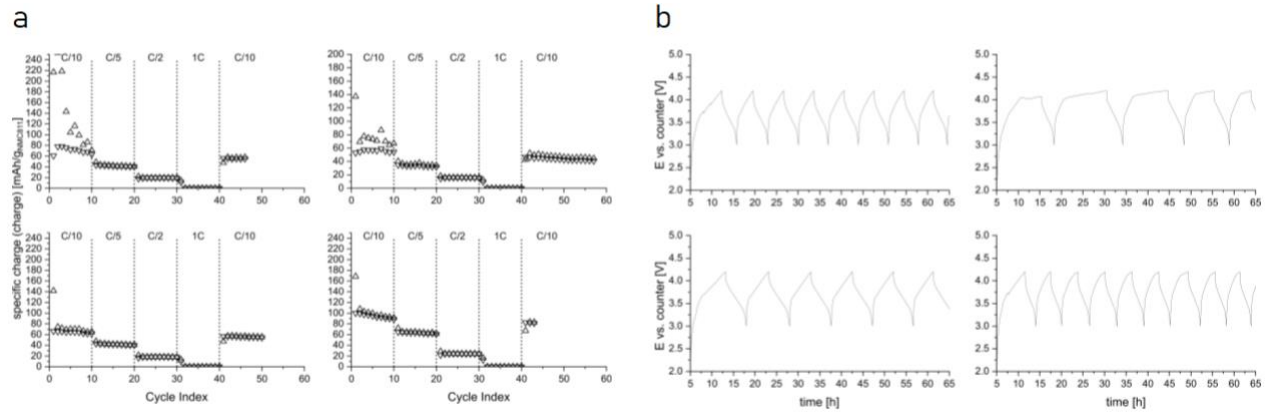

Figure 6. Rate capability tests of 4x 100 x 70 mm² pouch cells after hot-calendaring during cell assembly. GCPL at 3.0-4.2 V vs. Li^+/Li were used and C rates of C/10, C/5, C/2, 1C with respect to the nominal loading of the composite cathode (~1mAh/cm²).

2.5. SAFETY AND INFLUENCE OF MOISTURE

An HF sensor from Dräger (X-am 5100 EC HF/HCl) was used to measure potential HF release from the composite electrodes as well as precursor materials (e.g. electrode slurries). The results showed that no HF could be detected from the materials upon exposure to ambient air (25 °C, ~50-60% rel. hum.), see Table 5.

Furthermore, the influence of moisture on the electrochemical performance was tested. All three components of the cell, i.e. the composite anode, cathode, and gel electrolyte (SOLIFLY) were exposed to ambient air for 2 hours (~46 % rel. humidity). Then, they were introduced into a glovebox and assembled in coin cells. Figure 7 depicts the performance of this coin cells and shows the comparison to cells for which the components were not exposed to ambient air. No significant difference in terms of performance were obtained. Hence, it can be assumed that it

is safe to handle the components in ambient air which is especially important for the integration into the composite plates of the demonstrator.

Table 5. HF readings of different samples exposed to ambient air.

Sample	HF-sensor readings				
	1h	2h	5h	10h	24h
3M LiFSI in $PYR_{13}FSI$ (3 g)	0.0	0.0	0.0	0.0	0.0
3M LiFSI in $PYR_{13}FSI$ (20 g)	0.0	0.0	0.0	0.0	0.0
Anode slurry (100 g)	0.0	0.0	0.0	0.0	0.0
Cathode (70x100 mm^2)	0.0	0.0	0.0	0.0	0.0
Anode (70x100 mm^2)	0.0	0.0	0.0	0.0	0.0
Gel electrolyte (70x100 mm^2)	0.0	0.0	0.0	0.0	0.0

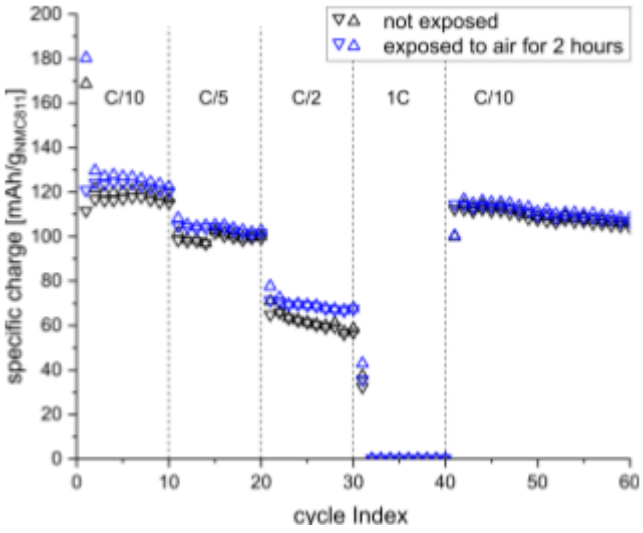

Figure 7. Performance comparison of cell components exposed or not exposed to the ambient air.

TGA-FTIR gas emission analysis was conducted on the assembled full-cells to further validate the safety of the developed system (Figure 8). A mass loss of around 3-4 wt.% was observed, starting at temperatures of around 100 °C. Similar weight losses were observed for all samples and the data seemed to be quite reproducible. The weight losses resulted in gas formation, which was further analysed by FTIR.

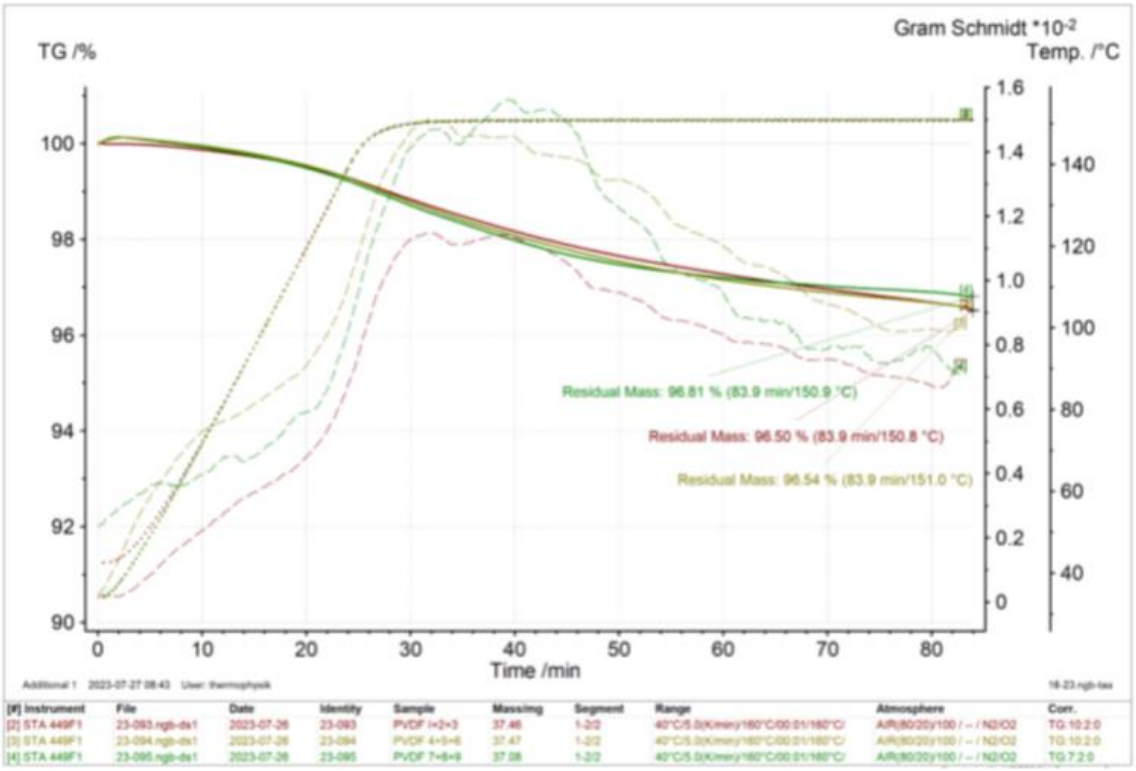

Figure 8. TG plot of three assembled cell samples.

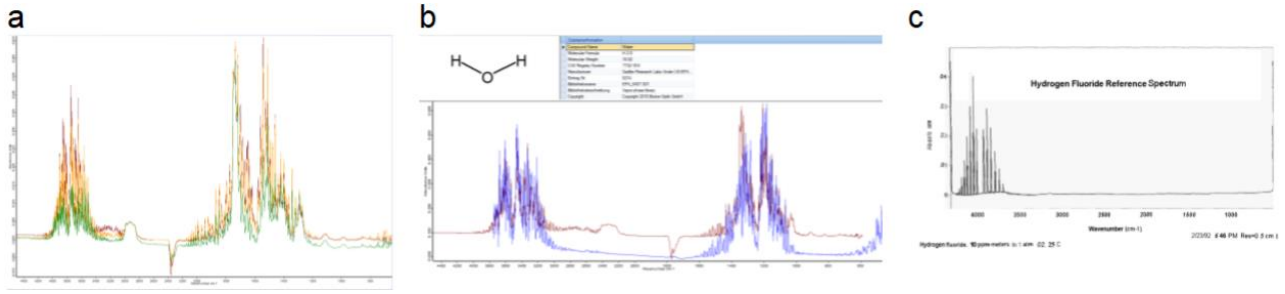

Figure 9. a, FTIR plots of all three samples; b, comparison of the measured signal with the expected signal for H_2O; c, expected signal for HF.

Figure 9 shows that mainly H_2O was released during heating of the full-cell assemblies. The characteristic peaks for HF could not be recorded, though, verifying the safety of handling and heating the developed cells. The moisture uptake of the samples might be due to some issues encountered with the dry room at AIT. More rigorous drying and storage of the materials will be considered to avoid excessive moisture uptake of the components.

3. ELECTROLYTE DEVELOPMENT (KIT-HIU)

3.1. PREPARATION OF THE SEMI-SOLID ELECTROLYTE

The combination of a ceramic phase, i.e. $Li_{1.3}Al_{0.3}Ti_{1.7}(PO_4)_3$ (LATP), a polymer (PVdF-TrFE), and an ionic-liquid as composite electrolyte ensures high thermal stability, greater mechanical strength, and suitable electrochemical performance. LATP/PVdF-TrFE hybrid membranes with different ratios of the polymer were prepared by a simple method displayed in Figure 10. A large hybrid membrane of 10 x 8 cm^2 could be easily realized.

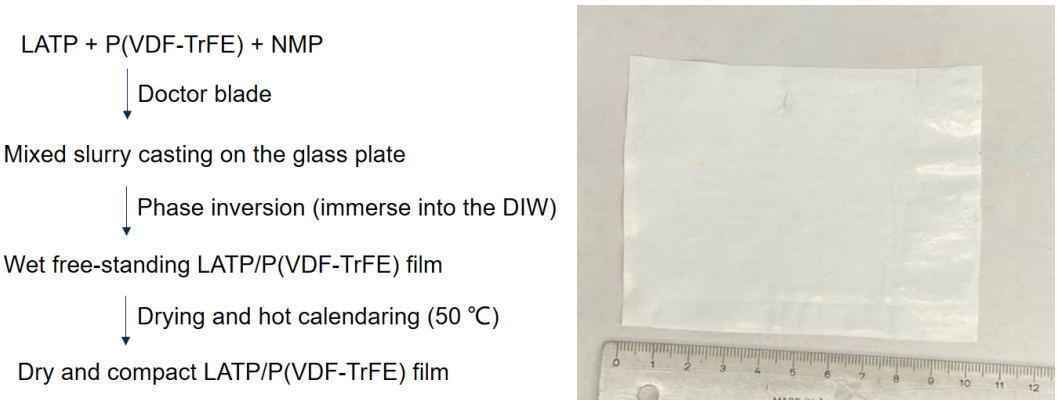

Figure 10. Preparation process and photograph of the LATP/PVdF-TrFE hybrid membranes.

Disks of 16 diameters were punched from the electrolyte membrane with different content of polymer. The membranes with 20 wt.% of polymer showed much better mechanical strength and less cracks after punching compared with the 8 wt.% sample (Figure 11 shows the surface structure of these two membranes). Accordingly, the hybrid membrane with 20 wt.% polymer was chosen for further testing.

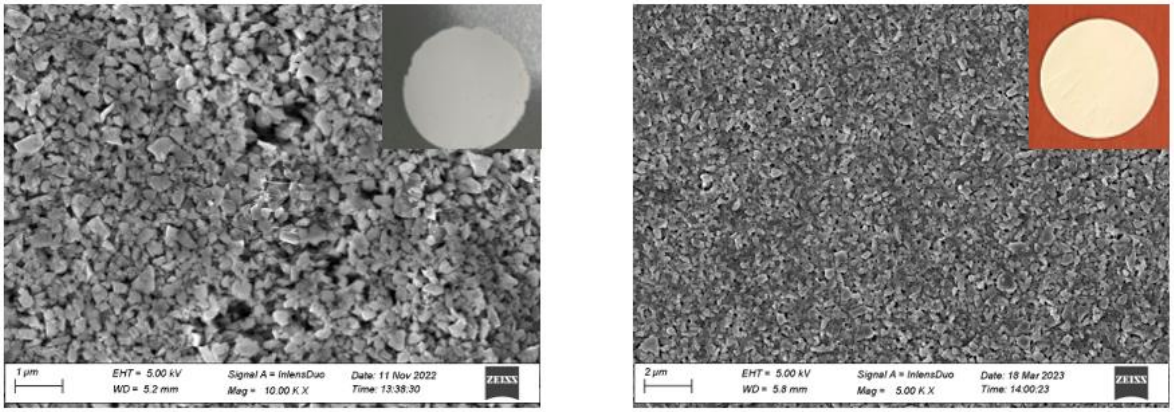

Figure 11. SEM images and photographs of the LATP/PVdF-TrFE membranes with 8 wt.% (left) and 20 wt.% (right) polymer.

N-Propyl-*N*-methylpyrrolidinium bis(fluorosulfonyl)imide ($Pyr_{13}FSI$) and 1-butyl-1-methylpyrrolidinium bis(fluorosulfonyl)imide ($Pyr_{14}FSI$) ionic liquids in combination with LiFSI and LiTFSI as lithium salts with a different molar ratio were used as the liquid electrolyte phase in the semi-solid electrolyte.

Table 6. Recipe of the electrolyte.

	LATP/PVdF-TrFE [wt.%]	3M LiFSI in $Pyr_{13}FSI$ [wt.%]
LATP/PVdF-TrFE/ionic liquid electrolyte	55 (with 80:20 LATP:PVdF-TrFE)	45

The assessment of the thermal stability of the ionic liquid-based electrolyte and the LATP/PVdF-TrFE hybrid membrane was conducted to ensure their compatibility with the stringent curing process demands of the carbon frame. As depicted in Figure 12, the DSC results of the ionic liquid-based electrolyte (3M LiFSI in $Pyr_{13}FSI$) revealed the absence of any significant heat variation or chemical reactions within the system, even when subjected to elevated temperatures of up to 160 °C. Figure 13 provides a visual representation of the *Celgard* and LATP/PVdF-TrFE membrane when exposed to a temperature of 160 °C. Notably, the LATP/PVdF-TrFE membrane exhibited a better shape retention and no sign of melting, which was in stark contrast to the *Celgard* membrane. This distinct behaviour ensures the prevention of cell short circuits due to the high-temperature battery sealing procedure.

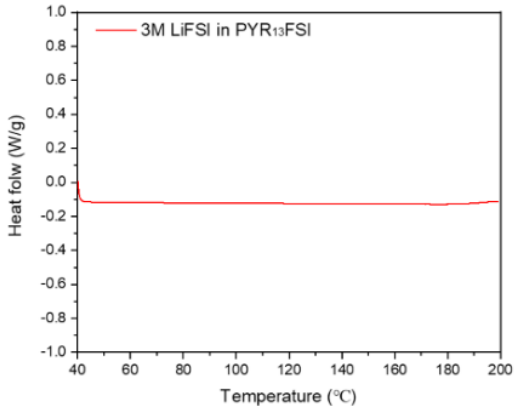

Figure 12. DSC testing of 3M LiFSI in $Pyr_{13}FSI$.

Figure 13. Photographs depicting the thermal testing of Celgard and the LATP/PVdF-TrFE membranes.

Then ~30 µL cm^{-2} of the ionic liquid-based electrolyte were added to the hybrid membranes. All the liquid was trapped by the hybrid membrane without any leakage. The obtained LATP/PVdF-TrFE/ionic-liquid semi-solid electrolyte showed an ionic conductivity of 0.67 mS cm^{-1} at 20 °C and 1.3 mS cm^{-1} at 40 °C, which is suitable for the battery operation, see Figure 14.

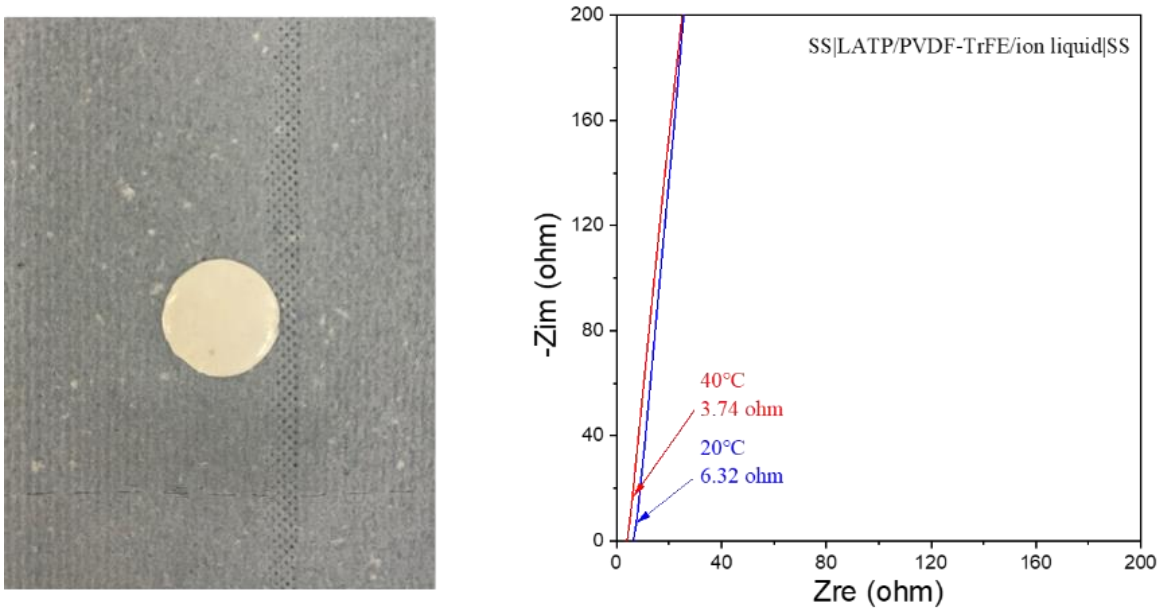

Figure 14. Photograph and EIS data recorded for the LATP/PVDF-TrFE/ionic-liquid semi-solid electrolyte.

3.2. ELECTROCHEMICAL MEASUREMENT OF FULL-CELLS

The electrochemical performance of the Si/C||NMC (electrode from AIT) full-cells with different electrolytes is reported in Figure 15. Around 125 mAh/g_{NMC811} were obtained for the first cycle when using the semi-solid electrolyte (Figure 16). Nevertheless, a poor Coulombic efficiency was observed and is assumed to result from the reduction of Ti^{4+} to Ti^{3+} at the anode|electrolyte interface.

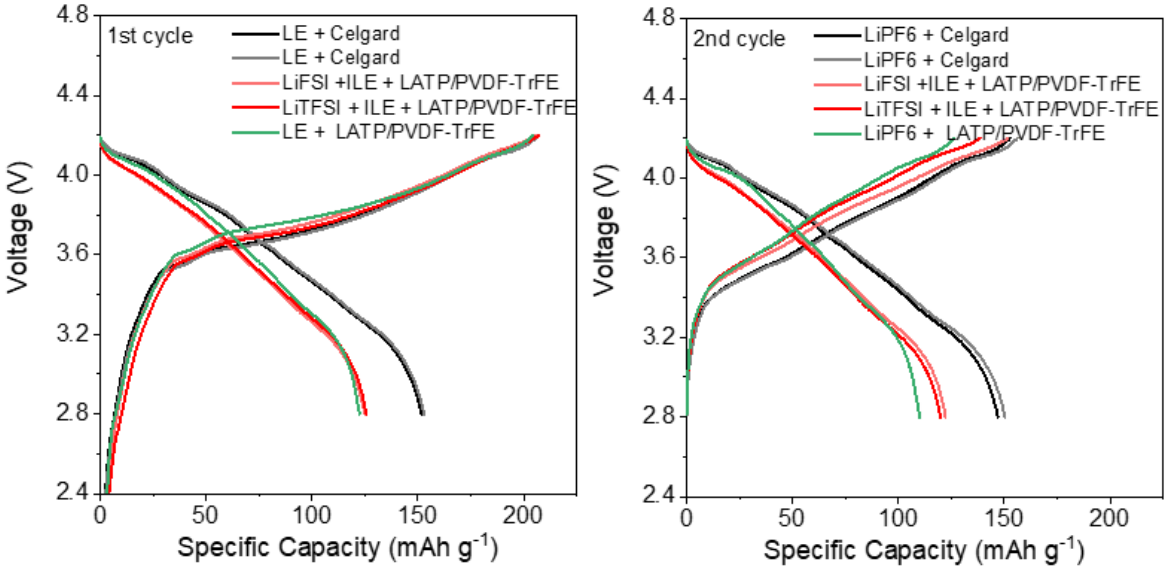

Figure 15. Dis-/charge profiles of Si/C||NMC full-cells employing different electrolytes.

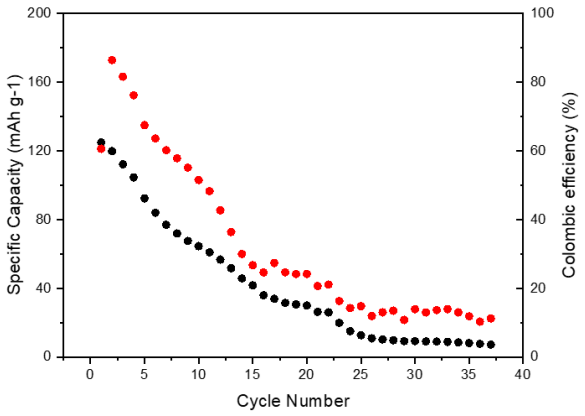

Figure 16. Cycling stability of an Si/C||NMC full-cell employing the semi-solid electrolyte.

Cyclic voltammetry experiments using a three-electrode setup also indicated some side reactions of the semi-solid electrolyte, see Figure 17a. The post-mortem analysis of some of the assembled cells (Figure 17b) showed that the cathodes were easily detached from the electrolyte film whereas the anodes usually stuck to it, probably because of the reaction at the anode|electrolyte interface.

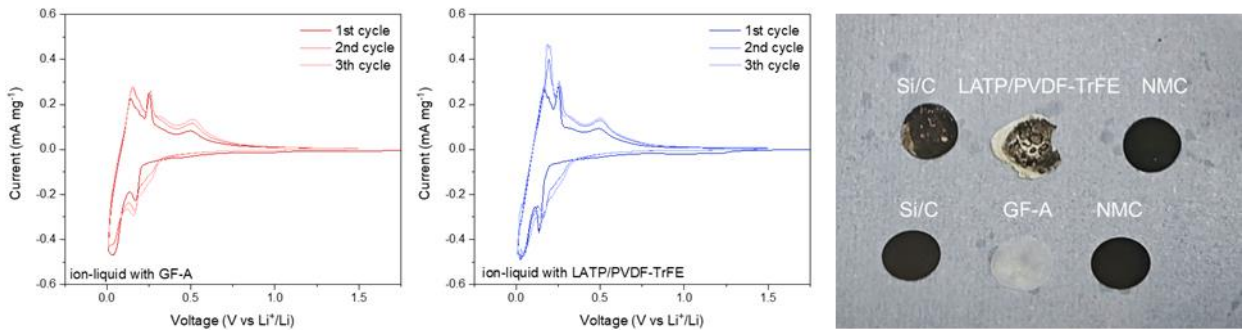

Figure 17. Cyclic voltammetry test of Si/C||NMC full-cells employing different electrolytes and photographs of the electrodes and electrolyte sheets after cycling.

3.3. ANODE PROTECTION

Therefore, a stabilizing interlayer resulting from the in-situ polymerization of 1,3 dioxolane (DOL) was introduced on the anode side (Figure 18). In addition, the developed process could reduce the volume expansion during lithiation and increase the adhesion between the electrolyte and the anode. $Al(OTF)_3$ was used as initiator for the polymerization process.

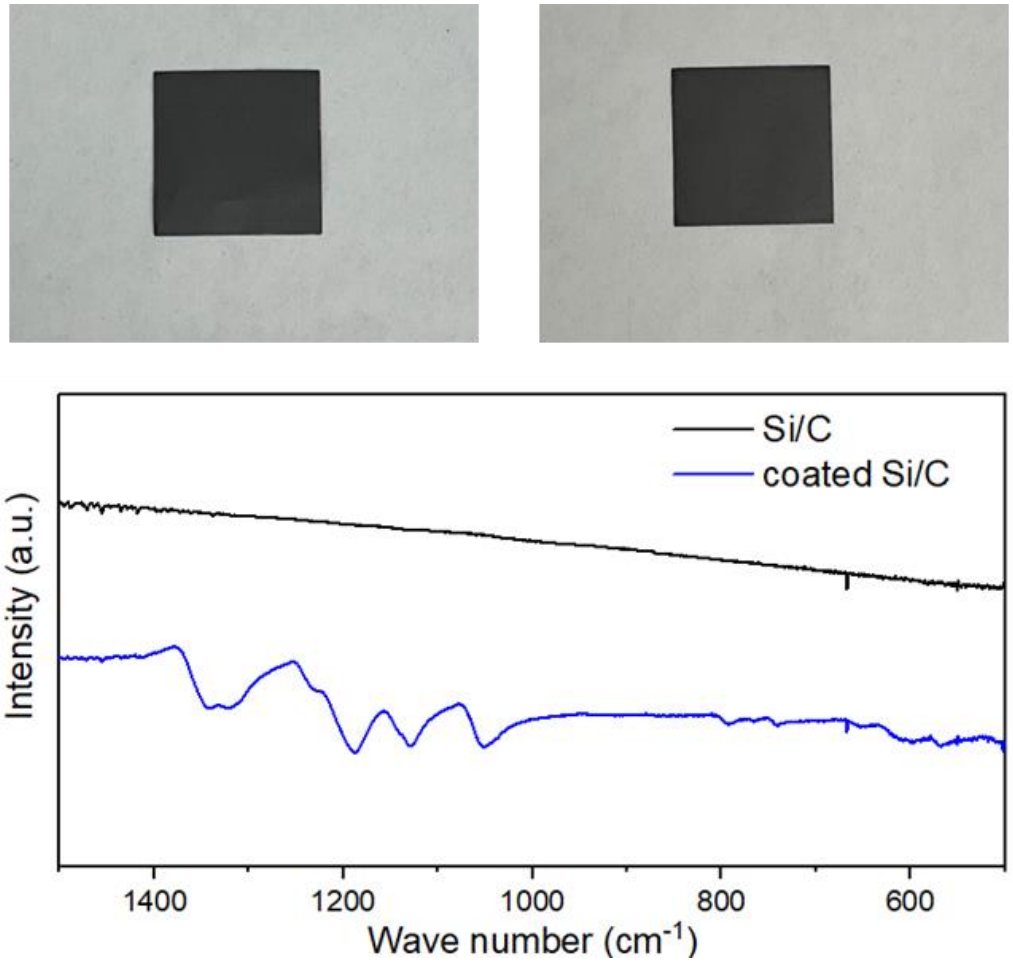

Figure 18. Photographs and FT-IR spectra of the pristine (left, black) and coated (right, blue) Si/C anode.

3.4. FULL-CELLS WITH A PROTECTED ANODE

The electrochemical performance of the Coated-Si/C||NMC full-cells comprising the semi-solid electrolyte is reported in Figure 19. Around 115 mAh/g_{NMC811} were obtained in the first cycle. The specific capacity of the cell was a little lower than the cell with the pristine anode, but its cycling stability was substantially improved. Also the cyclic voltammetry data revealed much less side reactions.

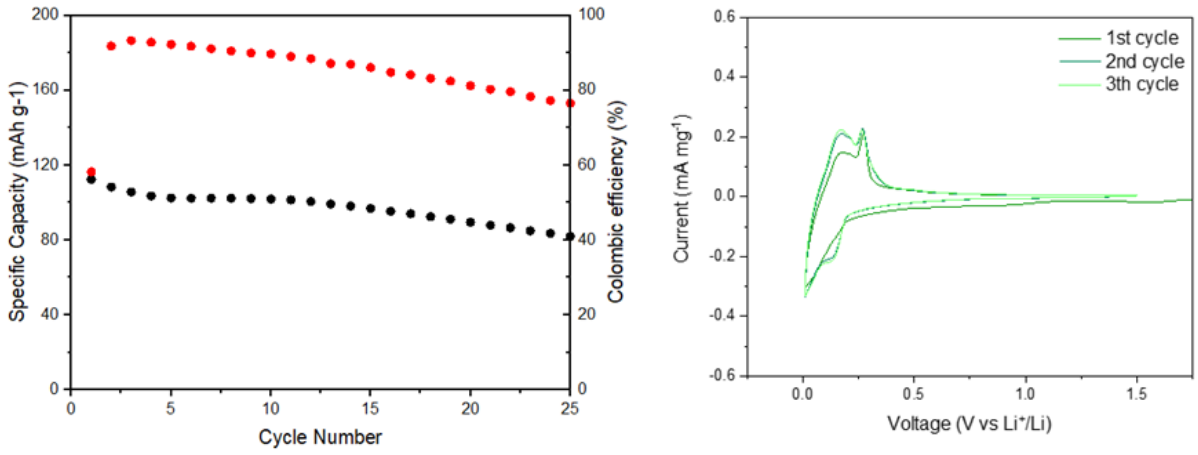

Figure 19. Galvanostatic cycling and cyclic voltammetry data recorded for Coated-Si/C||NMC full-cells comprising the semi-solid electrolyte.

4. MECHANICAL PROPERTIES (KIT-HIU)

To create composite structures that could share the load-bearing function with the structure and achieve an aircraft structural element capable of functioning as a battery, WP2 implemented electrode and electrolyte level design modifications.

4.1. ROBUST CERAMIC/POLYMER HYBRID ELECTROLYTE MEMBRANE

A ceramic/polymer composite structure was utilized for the electrolyte membrane to achieve a harmonious blend of strength and flexibility. This hybrid membrane harnesses the combined benefits of ceramics and polymers. In contrast to pure ceramics, the hybrid membrane exhibits superior flexibility, simplifying the cell assembly process and reducing susceptibility to damage subjected to loads in conjunction with other structural components in the aircraft wings. Moreover, in comparison to pure polymer electrolyte membranes, the incorporation of an 80 wt% high-strength LATP ceramic particle filler significantly enhances resistance to impact forces. Detailed mechanical properties parameters of the hybrid electrolyte membrane will be measured following the completion of later actions, which involve reducing the membrane's thickness and upscaling the producing process until we obtain the final product.

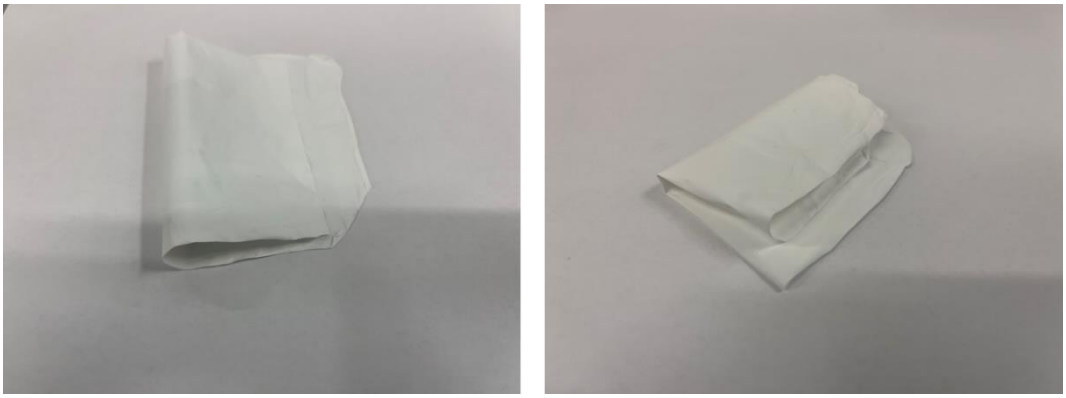

Figure 20. Photograph of flexible hybrid electrolyte membrane

4.2. BONDED ELECTRODES AND ELECTROLYTE

According to the simulation results from CIRA, it became evident that the solid laminates, as depicted in Figure 21 (and discussed in detail in deliverable D3.1), exhibited vulnerability to breakage during low-velocity/low-energy impact simulations. This susceptibility was anticipated to extend to our multi-layer-structure cells. Considering this finding, we made the decision to consolidate our multi-layer electrode/electrolyte/electrode cells into a single cohesive structure using the in-situ polymerization process mentioned earlier for the anode protection. As illustrated in Figure 22, the electrode coated with poly-DOL displayed a notable adhesive quality before the polymerization process reached full completion. By attaching the electrolyte membrane to this coated electrode, we could effectively bond multiple layers of electrodes and electrolytes together, creating an integral 'core' cell. This structure would significantly enhance the impact strength of the overall battery.

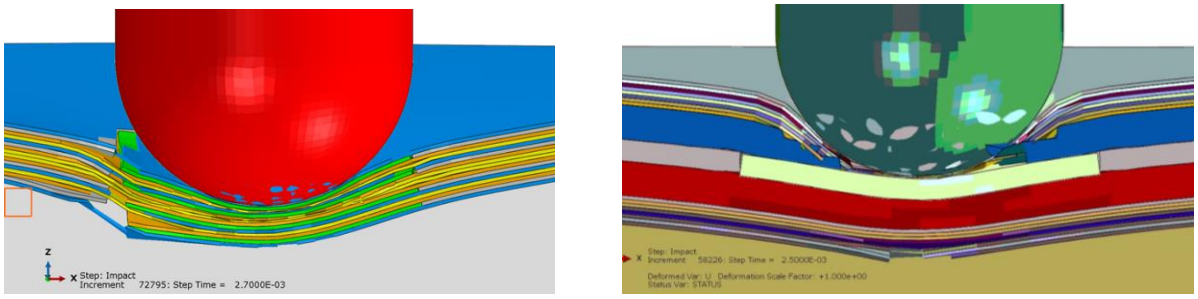

Figure 21. Preliminary simulation results of low velocity impact on solid laminates (left) and sandwich laminates with embedded battery (right)

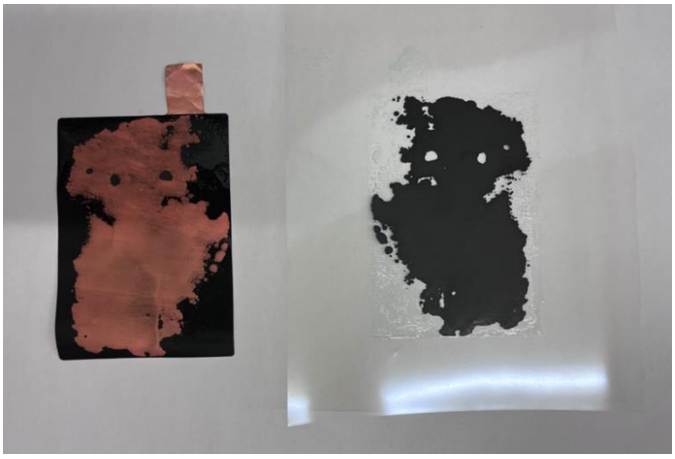

Figure 22. Photograph of sticky-coated electrode

5. CELL DESIGN (AIT)

5.1. ELECTRODE AND ELECTROLYTE DESIGN FOR POUCH CELLS

AIT proposed the electrode design depicted in Figure 23 for the first generation of pouch cells. The shape and position of the current collector tabs can be still modified-depending on the eventual needs for the sensors and processing.

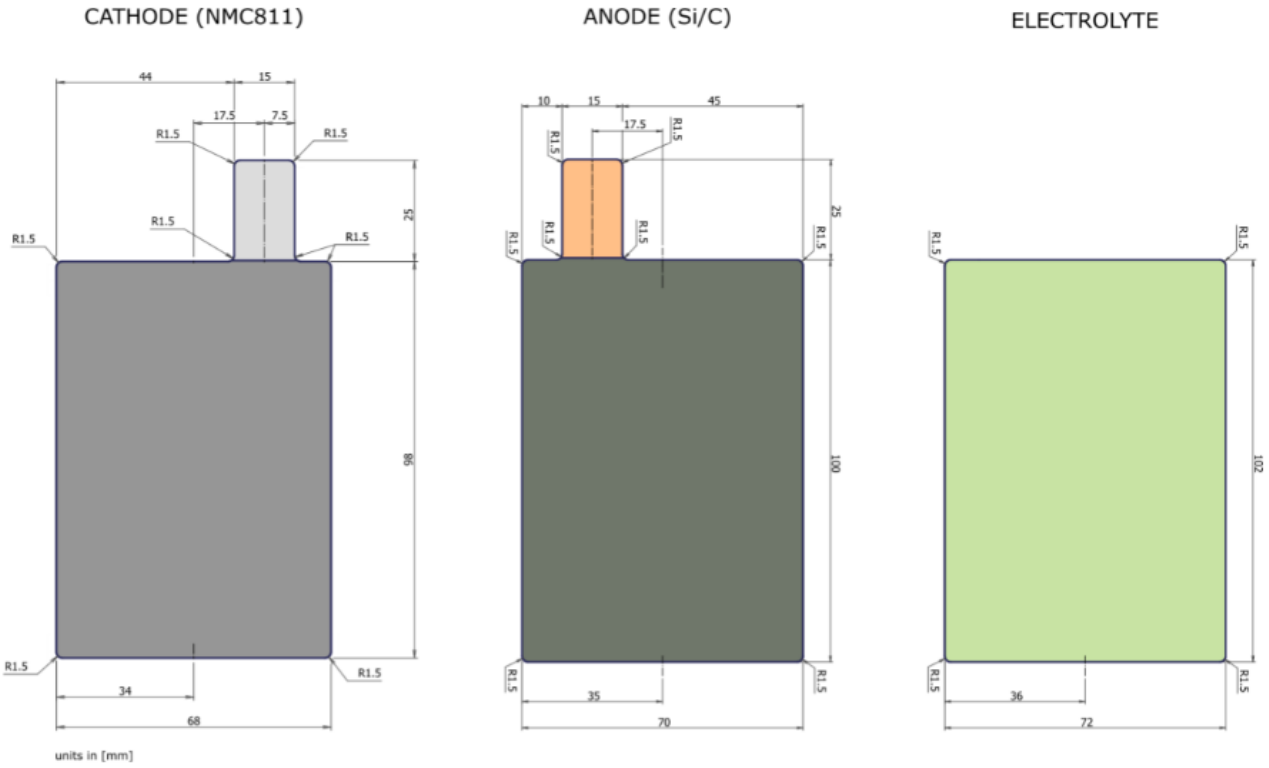

Figure 23. Cathode, anode, and electrolyte geometry for the first generation of pouch cells.

5.2. CAPACITY DESIGN FOR MULTI-LAYER POUCH CELLS

Following the reproducible assembly of coin cells and single-layer pouch cells, the materials prepared on the AIT pilot line were used to prepare multi-layer pouch cells. The initial electrochemical performance of three pouch cells with nominal capacities of 70 mAh (single layer), 140 mAh (double layer), and 280 mAh (4-layer) is shown in Figure 24. The specific charge values are comparable for all cells, showing no issues with assembly of the multilayer cells. The measured capacities of the cells are 35 mAh, 72 mAh, and 125 mAh, respectively.

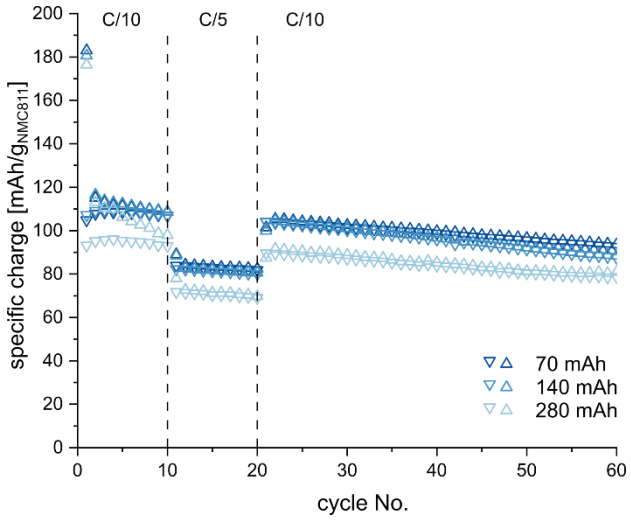

Figure 24. Initial electrochemical performance of single- (dark blue) and multi-layer (light blue) pouch cells.

Regarding the interim task of preparing 3x 700 mAh cells, a multi-layer cell with 23 electrode layers will be required. Thus, more work needs to be allocated to the improvement of the electrochemical performance to reduce the amount of layers and increase the energy density.

6. ON-CELL SENSOR DEVELOPMENT (SENSICHIPS)

The CMU-I is a double sided 100 µm thick polyimide foil where on one face is filled with copper to be then coated with anode electrode material and the other face holds electronics and sensors, see Figure 25, left. The active electronics side mounts the core SENSIPLUS smart sensor chip with few passive components to enable the EIS measurements, three thermistors located at the anode, cathode and very bottom of the foil and a large Interdigital Electrode (IDE), to measure structural bending and pressure.

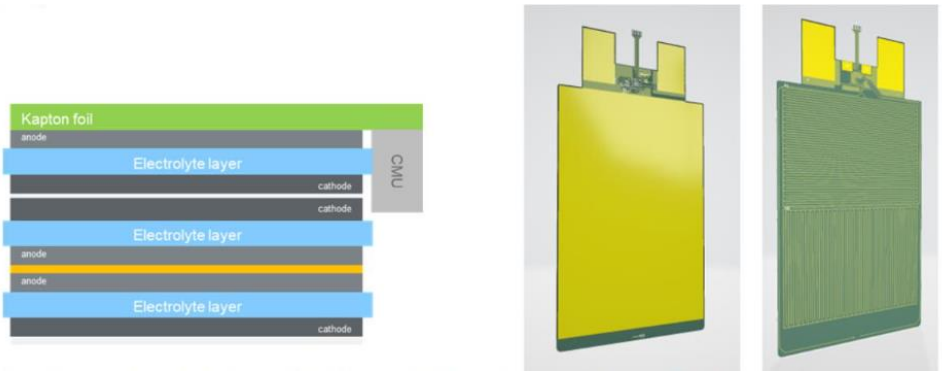

Figure 25. (Left) Battery layup including the CMU-I foil; (right) 3D model of the envisioned CMU-I unit. One side of the 100 µm thick CMU-I foil is filled with copper and coated to function as battery anode, the other side is holds the SENSIPLUS smart sensor chip along with thermal and structural sensors.

First we designed the electrical schematics and then performed the flex board layout, that consists in the components placing and wires routing, as shown in Figures 26 and 27.

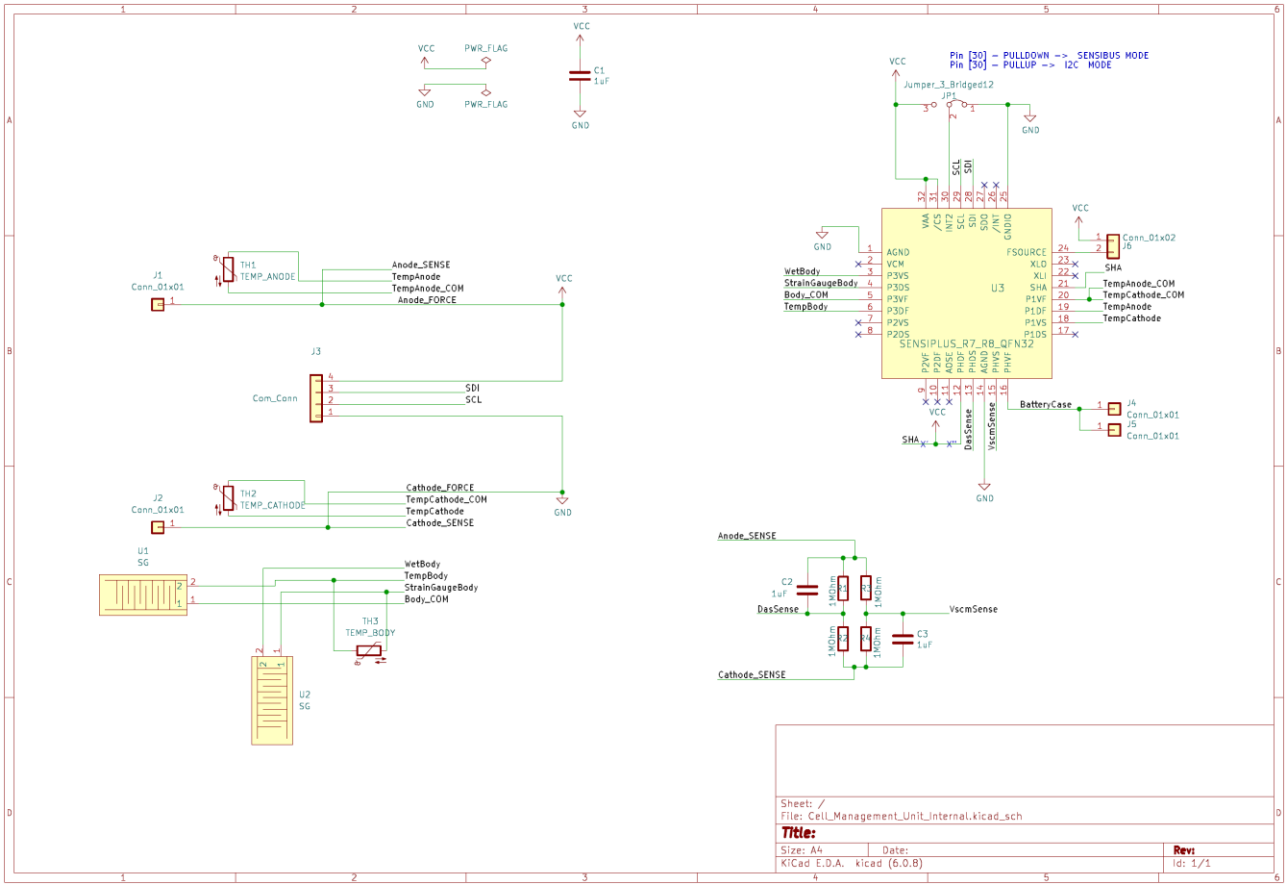

Figure 26. CMU-I electrical schematics.

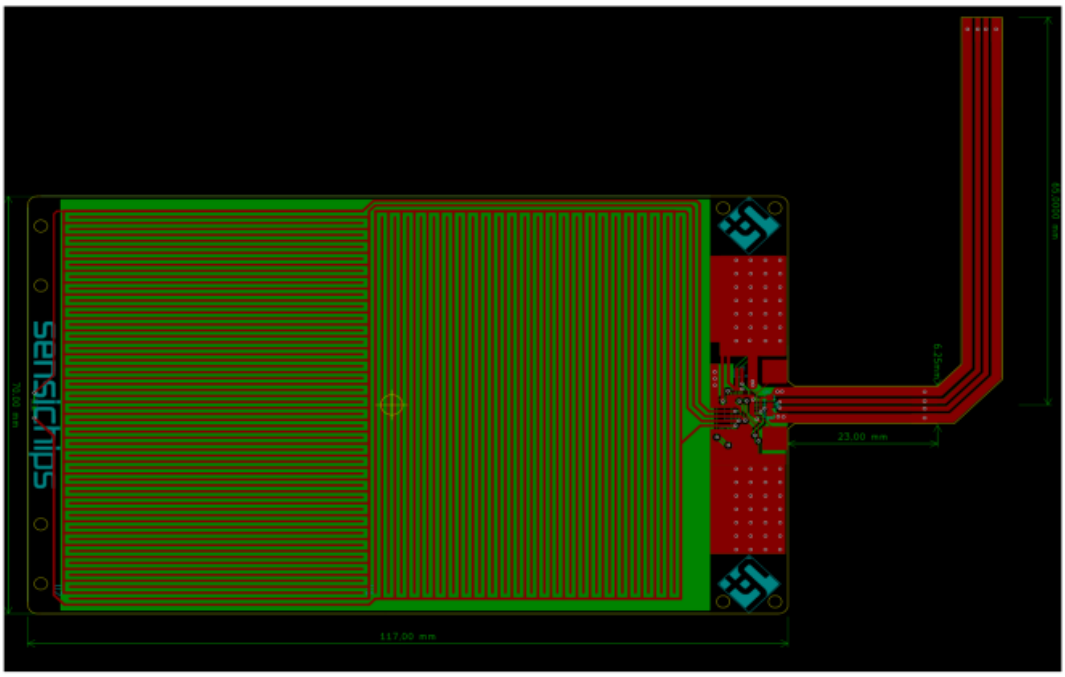

Figure 27. Final place and routing of the CMU-I flex board sent to manufacturing.

A 3D model of the envisioned design has been created and distributed among the partners see Figure 25, right.

102 CMU-I sheets have been fabricated, shipped to AIT (cf. Figure 28) and first tests of coating the CMU-I units with a composite anode layer were conducted.

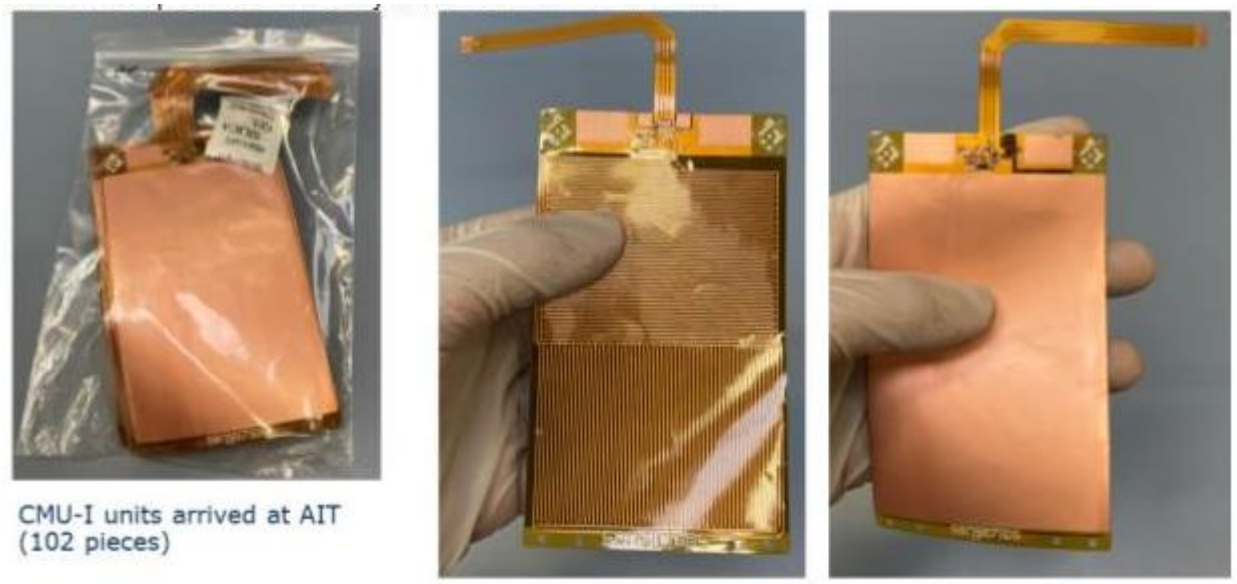

Figure 28. Photographs of the CMU-I units.

A first batch of 8 coated CMU-I layers was prepared at AIT and sent to SENSICHIPS for mounting of the electronics, see Figure 29. The coating layer was covered with a 10 µm thick polypropylene foil and each CMU-I unit was separately sealed under vacuum inside a dry room.

Assembly of the electronics components has just started at SENSICHIPS. The first step is to assembly the SENSIPLUS die (bare silicon die) with a wire bonding machine, and it is currently ongoing at GELCO SpA an external service company that has such specialized instrumentation. The die is sealed with an optically transparent resin cured at 120°C. The CMU-I flex with the assembled SENSIPLUS die is shipped to SENSICHIPS that will assemble the rest of the passive components and perform all required functional tests.

Figure 29. Left, coated CMU-I unit; middle, CMU-I unit after calendaring; right, CMU-I unit after calendaring and cleaning of the exposed leads.

7. SUMMARY

The present deliverable D2.1 reports the results obtained so far in Task 2.1, which focused on the electrochemical characterization of semi-solid full-cells, the up-scaling of the electrolyte and electrode preparation, and the integration of smart sensors.

A full screening of the different materials, developed during the project, was conducted. Firstly, different electrode materials and formulations, including the NMC cathode, the composite NMC cathode, the Si/C anode, and the composite graphite anode, were developed. Secondly, the compatibility of different compositions of ionic liquid-based electrolytes within the cell system was studied at the full-cell level with optimized electrodes. Finally, the full-cell harmonization of the different compounds was studied with different cell types.

The cycling test carried out on different electrodes and electrolytes system led to the following conclusions:

1) Both NMC||Si/C and composite NMC||composite graphite full-cells comprising the gel electrolyte showed good cycling stability and high specific capacity.

2) The LATP/PVdF-TrFE/ionic-liquid semi-solid electrolyte showed good thermal and mechanical stability, which is suitable for bearing structural loads and the high-temperature sealing process, as well as acceptable lithium-ion conductivity.

3) The compatibility of the LATP/PVdF-TrFE/ion-liquid semi-solid electrolyte in full-cells was relativity low, presumably owing to the reduction of Ti^{4+} to Ti^{3+} at the anode|electrolyte interface, which led to poor capacity retention of the full-cells.

4) The poly-DOL protection layer on the Si/C anode could reduce the side reactions between the electrode and the electrolyte, thus, improving the cycling stability. Further optimization of the protection layer is needed, though, to enable even higher capacities and enhanced Coulombic efficiency.

Additionally, the process of up-scaling electrodes and electrolytes was successfully carried out. Large electrode and electrolyte sheets (70 x 100 mm^2) were successfully produced for the multi-layer pouch cells. Batches weighing approximately 400 g each of the composite anode, composite cathode, and gel electrolyte were prepared for application on the AIT-pilot line. These batches were subsequently cast on surface-treated Cu foil and conventional Al foil for the composite anode and composite cathode, respectively. Furthermore, KIT has generated over 10 hybrid electrolyte sheets, which were subsequently forwarded to AIT for comprehensive electrochemical testing.

The outcomes of the reliability and scalability tests of the pouch cells with nominal capacities of 70 mAh (single layer), 140 mAh (double layer), and 280 mAh (4-layer), employing the scaled-up electrode and electrolyte components, have shown remarkable reproducibility and comparable electrochemical performance.

Moreover, the CMU-I foils, provided by SENSICHIPS, were coated with a composite graphite anode at AIT. Subsequently, these coated layers were sent back to SENSICHIPS for integration of the electronics. Assembly of electronics components is currently in progress at SENSICHIPS with the SENSIPLUS dies wire and bonding has just started. At completion of the components assembly, the board will be tested and characterized as a standalone device, meaning without the battery, and it will be shipped back to AIT for integration within the battery. The assembled battery with the CMU inside it, will be shipped back to SENSICHIPS for final testing.